JOURNAL OF CATALYSIS 1, 399-406 (1962)

# Diffusivity of Porous-Oxide-Gel–Derived Catalyst Particles

P. B. WEISZ AND A. B. SCHWARTZ

*From the Socony Mobil Oil Company, Inc., Research Department, Paulsboro, New Jersey*

Received April 30, 1962

For fifty-nine different samples of porous catalysts the effective diffusivities $D_{eff}$ have been measured. Results are compared with values calculated from pore volume and specific surface area in each case, on the basis of a random structure of cylindrical pores and also of a random structure of connecting cells. The latter model, suggested by a critical examination of the process of formation of the porous materials, results in satisfactory prediction of effective diffusivities of gel-derived catalysts. In pore structures having broad or bimodal pore size distributions actual values exceed the values thus calculated, and this result is shown to be inherent in the use of pore volume and surface area parameters to characterize an average pore property.

## INTRODUCTION

A previous paper (*1*) described a rapid method for the measurement of the effective diffusivity of cylindrically or spherically shaped porous catalyst particles. This paper deals with a study of effective diffusivities on nearly sixty different preparations of porous-oxide-gel–derived catalysts. It will be chiefly concerned with silica-aluminas subjected to various thermal and hydrothermal treatments. A few other gel-derived compositions including silica-magnesia and chromia-alumina are included for additional orientation. The measured diffusivities will be compared with those calculated from the pore size magnitude derived from surface area and pore volume data, and assuming a simple model of a "random pore structure" (*2*). The study allows conclusions to be drawn concerning the feasibility of making diffusivity estimates in the absence of direct measurement, and concerning the adequacy of the simple random pore model in describing diffusive flow properties of actual gel-derived structures. Included is an examination of the effect of a bimodal pore size distribution.

## EXPERIMENTAL

### 1. *Catalysts*

*Silica-alumina* catalysts used were conventional cracking catalyst beads. They are spherical particles of about 4 mm diameter, used in commercial cracking operations.

As previously described (*3*), a sodium silicate solution was mixed with a sulfuric acid-aluminum sulfate solution to form a quick-setting sol, droplets of which were dropped into oil to set into spheroidal hydrogel particles. The hydrogel beads were aged in hot water to control their density, ion-exchanged with an aluminum salt to replace zeolitic sodium, and water-washed.

Samples designated as silica-alumina (Cr) contain 0.15 wt % of chromia. Those without Cr addition are designated as "white."

Upon drying, the spheroidal hydrogel particles shrink by a factor of about 2.2 in diameter. When filled with a clear liquid (preferably of moderately high refractive index such as carbon tetrachloride or benzene) the dried and calcined particle is clearly transparent. They are considered to be "all embracive" gel structures, i.e. to form a continuous and nearly homogeneous pore structure.

Very dense gel structures can be obtained by reducing the severity or eliminating the hot aging of the freshly aged hydrogel. Samples of this type of catalyst are included (Samples #1, 2, 5, 33) in this study.

*Silica-magnesia catalysts* were made (*4*) by mixing a sodium silicate solution, a sulfuric acid solution, and a slurry of magnesia in water to form a suspension of magnesia in a silica sol, which was dropped into oil to set into spheroidal hydrogel particles. The hydrogel particles were aged in hot water, ion-exchanged with a magnesium salt solution, washed, dried and calcined.

*Chromia-alumina* samples were made (*5*) from a chromia-alumina hydrogel by mixing a sodium aluminate solution with a chromic acetate solution and allowing the resulting sol to flow into oil to set into spheroidal particles. The hydrogel particles were treated with an ammonium sulfate solution, washed, dried, and calcined. The chromia-alumina-molybdena catalyst was prepared by impregnation of the dried chromia-alumina gel with molybdena (*6*).

*Bimodal pore structures* were studied in the form of pelleted powders, and in the form of gel-derived particles wherein the macropore distribution was induced by inclusion of hard powders into the hydrogel during formation:

The silica-alumina macropore catalyst (Sample #54) was made in a similar manner as the silica-alumina catalyst (see above) except that pulverized dried silica-alumina was dispersed in the silica-alumina sol.

The silica-magnesia macropore-containing material (Samples #58, 59) was made in a similar manner as the silica-magnesia catalyst, except that pulverized dried silica-alumina gel was dispersed with the magnesia in the silica sol.

Chromia-alumina-molybdena (#57) consisted of abrasion fines of this material pressure pelleted into cylindrical shapes of ⅛ × ⅛ inch.

Two types of commercial clay cracking catalyst pellets manufactured by the Filtrol Corp. were examined. One (#56) was derived from montmorillonite, another (#55) from halloysite. Both had been used in commercial cracking operations, withdrawn from the unit, and examined in the regenerated (carbon-free) state.

Also, three of the "homogeneous" silica-alumina bead catalyst samples (Samples #34 to 37) were examined after having undergone extensive commercial cracking operations in three different cracking installations.

### 2. *Diffusivity Measurements*

Diffusivity was measured using the apparatus and method described by Weisz (*1*) based on the diffusion rate of hydrogen gas through a mounted particle into a stream of nitrogen gas, at room temperature and atmospheric pressure, and with no net pressure differential between the hydrogen- and nitrogen-bathed faces of the catalyst particle.

For each sample of catalyst, reported diffusivities constitute arithmetic averages of individual diffusivity tests, on at least 20 beads or pellets of each catalyst material.

### 3. *Structural Properties*

*The specific surface area, S,* was measured by nitrogen adsorption in a standard BET apparatus.

*The particle density,* $d_p$, represents the weight of the particle relative to the entire geometric volume of the spherical bead, or cylindrical pellet. It was obtained from measurements of the amount of displaced mercury when a known weight of catalyst material was immersed therein.

*The pore volume,* $p_v$, was obtained manometrically by determination of the volume of helium gas which fills a space containing a known weight of the catalyst sample with the volume corresponding to that of its geometric volume (based on $d_p$).

Pore volumina were also obtained by calculation from the particle density, $d_p$, and knowledge of the solid density of the solids composition $d_s$. For silica-alumina, $d_s = 2.30$, silica-magnesia, $d_s = 2.50$. The pore volume should be $p_v = 1/d_p - 1/d_s$.

Pore voluminas obtained by this calculation will be designated as $p'_v$.

## RESULTS AND DISCUSSION

Tables 1 and 2 summarize all pertinent experimental data which have been obtained, together with data concerning the origin of the various samples and sample types. Table 1 contains the data for all silica-alumina catalysts possessing an essentially homogeneous pore structure. Table 2 shows data on composition other than silica-alumina, and on catalyst particles possessing a bimodal pore size distribution.

### 1. *Calculation of Diffusivity from $p_v$ and S*

Wheeler (*2*) has discussed the diffusive properties of catalyst particles based on a model of random pores, i.e. pores which criss-cross each other in random directions.

With the possible exception of a portion of the pores in samples #54 to 59 having a bimodal pore size distribution, the pore diameters of all samples of this study are at most equal to (Sample #33) and usually far below 200 Å in dimension, i.e. appreciably smaller than the gaseous mean free path at atmospheric pressure which is of the order of 1000 Å. For the purposes of this study we can therefore assume the diffusivity in the *pore space* alone, $D_K$, to be the Knudsen diffusivity

$$D_K = \tfrac{2}{3}\bar{r}\bar{v} \qquad (1)$$

with $\bar{r}$ the pore radius, and $\bar{v}$ the kinetic velocity of the diffusing molecules, which we take as $\bar{v} = 1.75 \cdot 10^5$ cm/sec for hydrogen (*7*), the diffusing gas in the experimental determination.

If diffusion rates are based on total particle volume, this diffusion coefficient must be corrected by the fraction of pore space to total particle space, i.e. by multiplication with the porosity $\alpha$. Furthermore, it has been customary (*2*) to assume that the actual path length due to random criss-crossing of channels is greater than the particle dimension by $\sqrt{2}$. Thus

$$D_{\text{calc}} = \alpha(1/\sqrt{2})D_K = \tfrac{2}{3}(1/\sqrt{2})\alpha\bar{r}\bar{v} \qquad (2)$$

From (1) and (2) with $\alpha = d_p p_v$, and a pore radius as conventionally determined from $\bar{r} = 2p_v/S$, we obtain

$$D_{\text{calc}} = (1.64 \times 10^5)d_p p_v^2/S \qquad (3)$$

These calculated diffusivities are also tabulated in Tables 1 and 2 for each sample. The pore volume used was that measured by gas displacement, $p_v$, or was obtained from the density data and recorded as $p'_v$.

### 2. *Comparison of Measured and Calculated Diffusivities*

A comparison of the measured diffusivities and those calculated on the basis of the simple random pore model is made graphically in Fig. 1. Deviation from the predicted equality are represented by deviation from the solid diagonal line of unit slope.

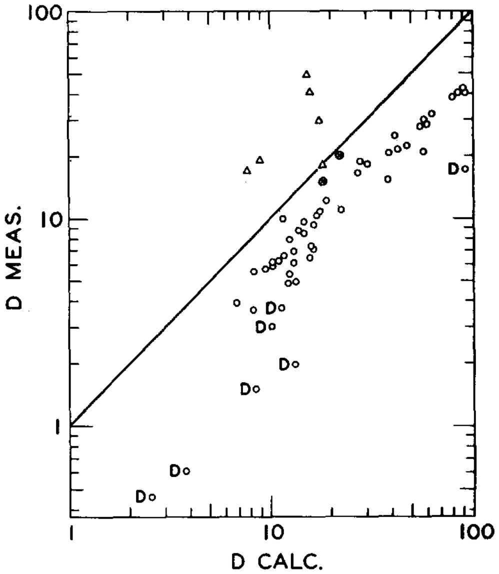

FIG. 1. Comparison of measured diffusivities with values calculated from conventional model of random cylindrical pores. (Samples Δ are special bimodal pore structures, samples marked D have unusually large particle densities).

We find that

(a) All points which present large deviations ($D_{\text{meas}} \leqslant .3\ D_{\text{calc}}$) are due to samples of high density (low porosity), (although not all samples of high density necessarily show large deviations).

## TABLE 1

### VARIOUS SILICA-ALUMINA MATERIALS POSSESSING AN ESSENTIALLY HOMOGENEOUS PORE STRUCTURE

| Silica-alumina beads (Cr) | | | Thermal treatment | | Hydrothermal (steam) treatment | | | $d_p$ (g/cc) | $p_v$ (cc/g) | $p'_v$ (cc/g) | $S$ (m²/g) | $D_{meas}$ (cm²/sec) | $D_{calc}$ (cm²/sec) |
|---|---|---|---|---|---|---|---|---|---|---|---|---|---|
| | | | T(°C) | Time | Time | T(°C) | $P_{atm}$ | | | | | | |
| 1 | Varied hot water treatment of hydrogel | | 705 | 3h | — | None | — | 1.50 | — | .24 | 381 | .6 | 3.7 |
| 2 | | | 705 | 3h | — | — | — | 1.26 | — | .36 | 409 | 3.9 | 6.6 |
| 3 | | | 705 | 3h | — | — | — | 1.15 | — | .44 | 455 | 5.6 | 8.0 |
| 4 | | | 705 | 3h | — | — | — | 1.03 | — | .54 | 433 | 9.9 | 11.3 |
| 5 | | | 705 | 3h | 24h | 650 | 1 | 1.56 | — | .21 | 135 | 1.5 | 8.3 |
| 6 | | | 705 | 3h | 24h | 650 | 1 | 1.33 | — | .32 | 188 | 4.8 | 11.9 |
| 7 | | | 705 | 3h | 24h | 650 | 1 | 1.29 | — | .34 | 192 | 6.1 | 12.7 |
| 8 | | | 705 | 3h | 24h | 650 | 1 | 1.22 | — | .39 | 194 | 7.4 | 15.6 |
| 9 | | | 705 | 3h | 24h | 650 | 1 | 1.15 | — | .44 | 216 | 10.1 | 16.7 |
| 10 | | | 705 | 3h | 24h | 650 | 1 | 1.10 | — | .48 | 221 | 12.1 | 18.6 |
| 11 | | | 705 | 24h | — | None | — | .92 | .57 | .66 | 250 | 8.7 | 13.7 |
| 12 | | | 705 | 24h | — | — | — | .99 | .50 | .58 | 244 | 7.1 | 16.2 |
| 13 | | | 705 | 24h | — | — | — | 1.07 | .43 | .50 | 230 | 5.4 | 12.2 |
| 14 | | | 705 | 24h | — | — | — | 1.16 | .35 | .43 | 210 | 3.7 | 10.3 |
| 15 | | | 705 | 24h | — | — | — | 1.20 | .32 | .40 | 201 | 3.0 | 10 |
| 16 | Varied hydrothermal treatment of dried gel | Vapor phase | None | | | None | | 1.06 | .470 | .51 | 377 | 5.9 | 10.2 |
| 17 | | | | | 2.2h | 650 | 3 | 1.22 | — | .39 | 190 | 8.4 | 14.4 |
| 18 | | | | | 8h | 232 | 20.5 | 1.06 | — | .51 | 82 | 27.4 | 55.5 |
| 19 | | | | | 16h | 224 | 20.5 | 1.04 | — | .52 | 74 | 31.8 | 63 |
| 20 | | | | | 5m | 282 | 67 | 1.07 | — | .50 | 114 | 20.8 | 38.5 |
| 21 | | | | | 1h | 306 | 68.5 | 1.07 | — | .50 | 49 | 40.1 | 90 |
| 22 | | | | | 5m | 375 | 68.5 | 1.07 | — | .50 | 105 | 21.5 | 42 |
| 23 | | Liquid phase | None | | 1h | 356 | 68.5 | 1.08 | — | .49 | 49 | 40.9 | 87 |
| 24 | | | | | 1h | 461 | 68.5 | 1.08 | — | .49 | 72 | 28.0 | 59 |
| 25 | | | | | 2m | 291 | 68.5 | .98 | — | .58 | 203 | 16.5 | 26.5 |
| 26 | | | | | 8m | 291 | 68.5 | .98 | — | .58 | 132 | 25.0 | 41.5 |
| 27 | | | | | 1m | 340 | 137 | .97 | — | .60 | 100 | 29.9 | 57 |
| 28 | | | | | 8m | 341 | 137 | .98 | — | .58 | 80 | 38.4 | 70 |
| 29 | | | | | 5h | 371 | 35 | 1.18 | — | .42 | 72 | 22 | 46.5 |

| | | | | | | | | | | | | |
|---|---|---|---|---|---|---|---|---|---|---|---|---|
| 30 | Low density beads hydrothermally treated | 650 | 10h | — | — | — | .84 | — | .76 | 285 | 18.7 | 28 |
| 31 | | — | — | 5h | 701 | 1 | 1.10 | — | .47 | 233 | 10.7 | 17.1 |
| 32 | | — | — | 1h | 292 | 20.5 | 1.12 | — | .46 | 176 | 10.8 | 22 |
| 33 | High density bead, hydr. tr. | — | — | 4h | 350 | 68.5 | 1.44 | — | .26 | 22 | 17.5 | 92 |
| 34 | From Beaumont, Tex. A | — | — | — | — | — | 1.32 | — | .33 | 195 | 7.9 | 12.1 |
| 35 | commercial Beaumont, Tex. B | — | — | — | — | — | 1.25 | — | .37 | 174 | 9.2 | 16.2 |
| 36 | cracking Augusta, Kan. C | — | — | — | — | — | 1.22 | — | .39 | 215 | 9.6 | 14.2 |
| 37 | units, used Augusta, Kan. D | — | — | — | — | — | 1.23 | — | .38 | 272 | 6.1 | 10.8 |
| 38 | Varied hydrothermal treatments, tempered in atm stream at 650°C, 10 hr | — | — | 1h | 204 | 17 | 1.17 | .35 | .42 | 152 | 6.4 | 15.4 |
| 39 | | — | — | 1h | 260 | 50 | 1.14 | .37 | .44 | 67 | 15.5 | 38 |
| 40 | | — | — | 6h | 260 | 55 | 1.10 | .40 | .47 | 46 | 20.3 | 57 |
| 41 | Various hydrothermal treatment untempered | — | — | 5m | 354 | 68.5 | .99 | .50 | .58 | 134 | 18.6 | 30 |
| 42 | | — | — | 1h | 354 | 68.5 | .99 | .50 | .58 | 46 | 42.2 | 89 |
| 43 | Thermal deactivation series | 540 | 16h | — | — | — | 1.07 | .412 | .50 | 366 | 5.5 | 8.2 |
| 44 | | 593 | 16h | — | — | — | 1.06 | .412 | .51 | 352 | 6.2 | 8.3 |
| 45 | | 650 | 16h | — | — | — | 1.08 | .398 | .49 | 304 | 5.7 | 9.2 |
| 46 | | 705 | 16h | — | — | — | 1.12 | .381 | .46 | 269 | 6.0 | 10 |
| 47 | | 760 | 16h | — | — | — | 1.15 | .345 | .43 | 196 | 6.6 | 11.5 |
| 48 | | 815 | 16h | — | — | — | 1.20 | .317 | .40 | 153 | 7.0 | 12.8 |
| 49 | | 870 | 16h | — | — | — | 1.28 | .250 | .36 | 98 | 4.9 | 13.3 |
| 50 | | 925 | 16h | — | — | — | 1.59 | .121 | .20 | 29 | 1.9 | 13.3 |

TABLE 2

VARIOUS NON-SILICA-ALUMINA MATERIALS OF HOMOGENEOUS PORE STRUCTURE, AND SILICA-ALUMINA CATALYSTS HAVING BIMODAL PORE SIZE DISTRIBUTION

| | Thermal treatment | | Hydrothermal (steam) treatment | | | $d_p$ (g/cc) | $p_v$ (cc/g) | $p'_v$ (cc/g) | $S$ (m²/g) | $D_{meas}$ (cm²/sec) | $D_{calc}$ (cm²/sec) |
|---|---|---|---|---|---|---|---|---|---|---|---|
| | T(°C) | Time | Time | T(°C) | $P_{atm}$ | | | | | | |
| *Other homogeneous catalyst compositions* | | | | | | | | | | | |
| 51 Silica-magnesia (HT 4500) beads | — | — | — | — | — | 1.71 | .201 | — | 442 | .45 | 2.6 |
| 52 Chromia-alumina (CA 3452) beads | — | — | — | — | — | 1.60 | .368 | — | 162 | 20 | 22 |
| 53 Chromia-alumina-molybdena (CA 3487) beads | — | — | — | — | — | 1.75 | .310 | — | 155 | 15 | 18 |
| *Bimodal pore size particles* | | | | | | | | | | | |
| 54 Silica-alumina macroporous beads (LC 1961) | 790 | 3h | — | — | — | .96 | .61 | — | 376 | 49 | 15.2 |
| 55 SR Clay pellets—from commercial crack. unit | — | — | — | — | — | 1.01 | .26 | — | 65 | 29 | 17.1 |
| 56 "A" Clay pellets—from commercial crack. unit | — | — | — | — | — | .90 | — | .33 | 105 | 42 | 15.4 |
| 57 Chromia-alumina-molybdena, pelleted fines | — | — | — | — | — | 1.91 | .27 | — | 128 | 18 | 18.0 |
| 59 Silica-magnesia macroporous beads | 650 | 3h | — | — | — | 1.22 | — | .42 | 472 | 17 | 7.5 |
| 59 Silica-magnesia macroporous beads | 650 | 3h | 24h | 650 | 1 | 1.28 | — | .38 | 348 | 19 | 8.6 |

(b) With the exception of the abnormal high density samples, the observed diffusivities of the homogeneous silicate gels cluster generally around values approximately one-half those calculated from $\bar{r} = 2p_v/S$, with formula (3).

(c) Catalyst samples having a macropore structure (Table 2) superimposed on their micropore structure have diffusivities in excess of values calculated from the average pore radius based on $2p_v/S$.

### 3. *Adequacy of Simple Random Pore Model*

The formulation of the simple random pore model is guided by the tacit concept of empty pores piercing like empty tubes through otherwise *solid space.* It is noteworthy to reflect on the process of gel formation: Contrary to the above concept it should be visualized as *solid material,* growing from random point nuclei, *piercing* through otherwise *empty space.* It becomes more plausible to picture the resulting structure as consisting of overlapping "cells" rather than a structure of tubular pores. The cells are visualized as cubes or spheres, and for a given porosity $\alpha$, only a fraction $\alpha$ of the surface defining each cell will be "open" to a neighboring cell space. The position of the open surface will furthermore be randomly oriented in space. We then consider the following three points:

(a) The diffusional process may be conveniently pictured as a random walk from cell unit to cell unit. The process which normally leads to a diffusion coefficient $D_K = \frac{2}{3}\,\bar{v}\bar{r}$ must then be modified by lowering the probability for *successful* progress of each random step by $\alpha$, which now measures the fraction of the number of randomly directed "tries" which will get through each hypothetical cell surface. Thus we have the modified diffusion coefficient $D_K = \alpha\,\frac{2}{3}\,\bar{v}\bar{r}$ in place of Eq. (1).

(b) Since the model involves near-spherical rather than tubular pore spaces, the relationship of volume to surface should be better described by $\bar{r} = 3p_v/S$.

(c) We take the total correction of diffusion length as $\sqrt{3}$ (instead of $\sqrt{2}$) corresponding to the vector resulting from the addition of the *three* directional unit vectors of three-dimensional space. We thus obtain

$$D_{\text{calc}} = \tfrac{2}{3}(1/\sqrt{3})\alpha^2\bar{r}\bar{v}$$

in place of Eq. (2), or

$$D_{\text{calc}} = (2.14 \cdot 10^5)d_p{}^2p_v{}^3/S \qquad (4)$$

Figure 2 shows the set of experimental data plotted against the values calculated from the revised random cell model Eq. (4). The data average closely about the calculated line, and the effect of the correction by $(d_pp_v)$ has resulted in considerable narrowing of the total spread. This is true for all of the "homogeneous" catalysts. Only the catalysts with superimposed micro- and macropore structures remain to form a separate set of points (triangles) wherein $D_{\text{meas}} > D_{\text{calc}}$.

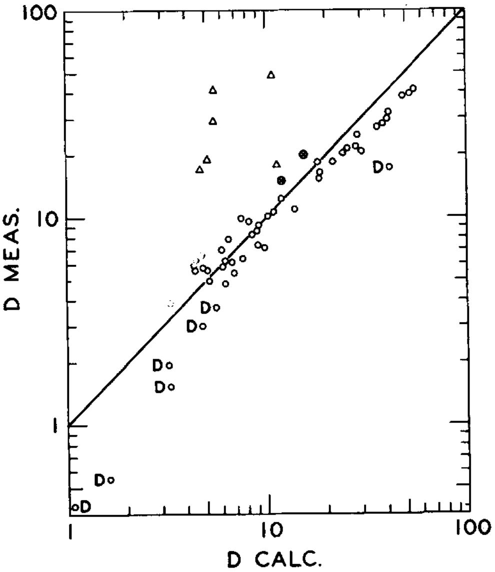

FIG. 2. Comparison of measured diffusivities with values calculated from modified model based on a structure of connecting cellular spaces. (Samples Δ are special bimodal pore structures, samples marked D have unusually large particle densities).

Catalyst samples showing the largest deviation from calculated diffusivities are those with abnormally high density, which have been marked "D." The existence of large numbers of pore constrictions would be expected to cause a depression in effective diffusivities; yet mere constrictions tending to obstruct but not close off pore spaces would not appreciably alter specific surface areas or pore volumina, as compared to a normal structure. In fact, we may take the ratio of $D_{\text{meas}}/D_{\text{calc}}$ as an indicator of or even a measure for the extent of pore space blockage.

### $D_{\text{meas}} > D_{\text{calc}}$ *for Broad Pore Size Distribution*

The diffusivities of catalysts with a significantly broad distribution in pore magnitudes consistently exceed the values calculated on the basis of an average pore radius $\bar{r} = 2p_v/S$, or $\bar{r} = 3p_v/S$.

It is possible to show that the observation $D_{\text{meas}} \geqslant D_{\text{calc}}$ is a necessary consequence when a broad pore size distribution exists:

For parallel cylindrical pores—as the simplest mathematical model for illustration—consisting of a distribution of $n_i$ pores per unit area of pores of $r_i$ radius, the effective measured diffusivity for a unit volume element of material would be

$$D_{\text{meas}} = \Sigma \tfrac{2}{3} \bar{v} a_i r_i n_i$$

where $a_i$ is the cross-sectional area contributed by the $i^{\text{th}}$ pore. Since $a_i = \pi r_i^2$, and the porosity $\alpha = \Sigma \pi r_i^2 n_i$, we can write

$$D_{\text{meas}} = \tfrac{2}{3} \bar{v} \alpha \frac{\Sigma r_i^3 n_i}{\Sigma r_i^2 n_i} \tag{5}$$

On the other hand

$$\frac{2p_v}{S} = \frac{2\Sigma \pi r_i^2 n_i l}{\Sigma 2\pi r_i l} = \frac{\Sigma r_i^2 n_i}{\Sigma r_i n_i} = \bar{r}$$

is used in Eqs. (1) and (2) to calculate diffusivity from pore volume and surface area data, i.e.

$$D_{\text{calc}} = 2\bar{v}\alpha \frac{\Sigma r_i^2 n_i}{\Sigma r_i n_i} \tag{6}$$

[leaving out $\sqrt{2}$ from Eq. (1) since the pores are straight in this model]. The observations, will be explained if we can show that Eq. (5) is necessarily greater than Eq. (6), i.e. if

$$\Sigma r_i^3 n_i \cdot \Sigma r_i n_i \geqslant [\Sigma r_i^2 n_i]^2 \tag{7}$$

Now, $\mu^{(\nu)} = \Sigma r_i^{(\nu)} n_i$ defines the $\nu^{\text{th}}$ absolute moment of the distribution in pore sizes. It is a well-known inequality theorem (*8*) that, for any distribution of properties, $\mu^{(\nu+1)} \cdot \mu^{(\nu-1)} \geqslant (\mu^{\nu})^2$ which is identical with Eq. (7), with $\nu = 2$. The observation is therefore proven to follow as a matter of mathematical necessity.

## CONCLUSION

Reasonable estimates of effective diffusivity of homogeneous oxide-gel–derived catalysts can be made from knowledge of pore volume and specific surface area, on the basis of a model of cellular pore spaces. Broad or bimodal distributions in pore size will lead to low estimates.

## REFERENCES

*1.* WEISZ, P. B., *Z. physik. Chem.* (*Frankfurt*) **11,** 1 (1957).

*2.* WHEELER, A., *Advances in Catalysis* **3,** 248 (1951).

*3.* PORTER, R. W., *Chem. Met. Eng.* **53,** 138 (1946).

*4.* SCHWARTZ, A. B., U. S. Patent 2,796,409.

*5.* STOVER, W. A., AND WILSON, R. C., JR., U. S. Patents 2,773,839 and 2,773,845.

*6.* STOVER, W. A., U. S. Patent 2,773,846.

*7.* "Handbook of Chemistry and Physics," 43rd ed., p. 3430. Chem. Rubber Publ. Co., 1961/2.

*8.* CRAMER, H., "Mathematical Methods of Statistics," p. 176. Princeton University Press, Princeton, 1951.